Smart Refractory Sensors Development for Corrosion and Erosion Monitoring in High Temperature Systems

Javier A. Mena[1], Katarzyna Sabolsky[1], Michael Jones[1], Nick Winch[1], Konstantino Sierros[1], Edward M. Sabolsky[1], Charity Stepp[1], Margaret Raughley[2]

[1]Department of Mechanical and Aerospace Engineering,
West Virginia University, Morgantown, WV 26506, USA

[2]Harbison Walker International, Inc

ECS 243rd Meeting Presentation May 30th
Corrosion Science and Technology

West Virginia University.

Introduction

- Processes such as energy generation, metals/glass manufacturing, coal gasification and aerospace technology applications require health and process monitoring in harsh-environments.
- **Harsh-environments conditions include:**
  - High temperature (500-1800^{o}C)
  - High pressure (up to 1000 psi)
  - **Corrosive, erosive and reducing environments.**
- **Ability to monitor:**
  - Temperature
  - Structural stability of systems components.

- **US DOE Overall Goal:** Develop health and temperature sensors (and sensor arrays) embedded into refractory compositions.

Objectives of This Work

- Synthesize conductive refractory lanthanum oxides perovskites using the Pechini Sol-Gel method.

- Study the electrical conductivity and Seebeck coefficients of such compositions at high temperatures and under different working atmospheres (oxidizing, reducing).

- Fabricate surface printed thick-film sensors utilizing these materials and test at high-temperature.

- Fabricate sensors embedded into refractory and perform thermoelectrical and corrosion testing.

Lanthanum Chromite: General Aspects

- High melting point (~2500 °C).
- Chemically stable under oxidative and reducing atmospheres.
- Pure $LaCrO_3$ shows semiconducting behavior with no to low ionic conduction.
- Calcium substitution increase conductivity from 1.0 to 40.0 S·cm^2 at 1000°C (Mori *et al.* 1997)
- Compatibility (thermal expansion coefficients matching) near refractory materials, ~10×10^{-6} $^{o}C^{-1}$.

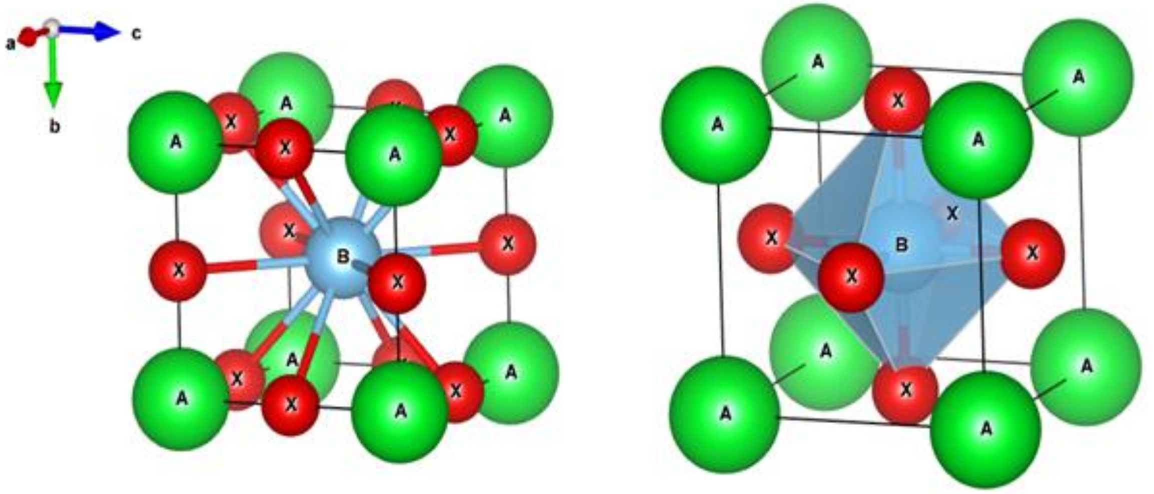

A atom cubic unit cell *B atom cubic unit cell*

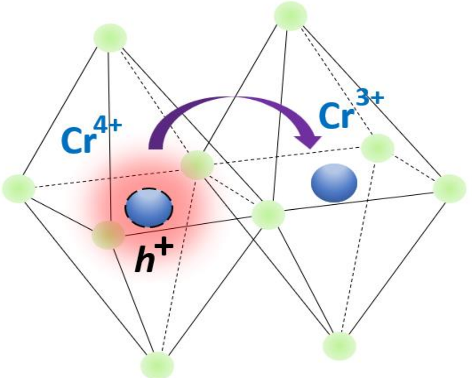

Polaron hopping electrical conduction

Sol Gel Synthesis and Pellet Fabrication

$La(NO_3)_3 6H_2O$ | $Sr(NO_3)_2$ | $Cr(NO_3)_3 9H_2O$

Citric Acid

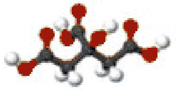

Mixing/Complex

Sol

Dried 80^{o}C

Gel

Calcination 900^{o}C

Powder

Reactive Sinter

Pellet

Heat treatment @ 1600^{o}C – 2 Hours

High density ceramic pellet

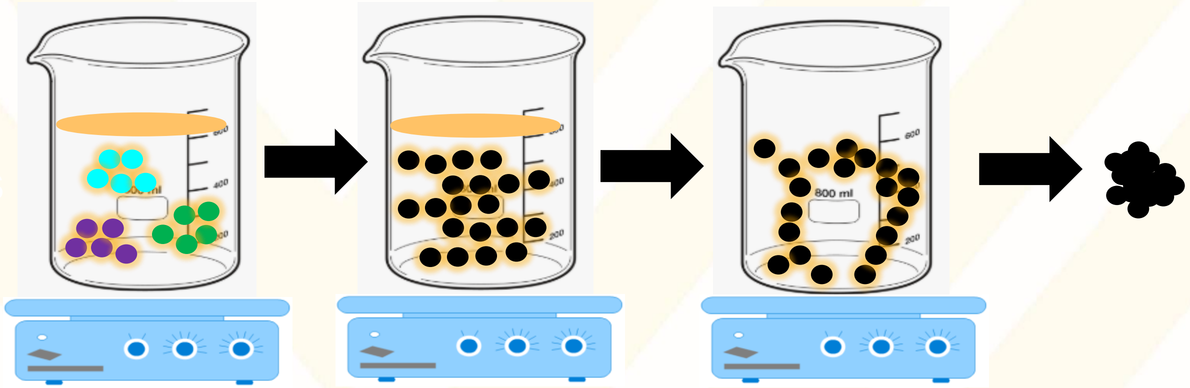

- ✓ Pechini-like process used.
- ✓ High homogenous and adequate sintering.
- ✓ High density (typical in literature <93% density).
- 🚫 Low yields and not easy to scale-up

<u>Compositions Studied:</u>

A-site: $La_{1-x}\mathbf{Sr}_xCrO_3$, $La_{1-x}\mathbf{Ca}_xCrO_3$

(x = 0.1, 0.2, 0.3, 0.4)

B-site: $La_{0.8}Sr_{0.2}Cr_{1-y}\mathbf{Mn}_yO_3$

(y = 0.1, 0.2, 0.3, 0.4)

Electrical Conductivity Characterization

DC Electrical Conductivity (Oxidizing Atmosphere)

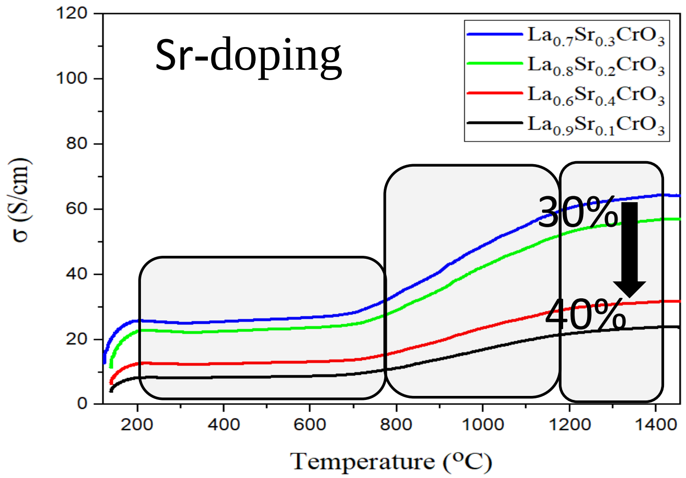

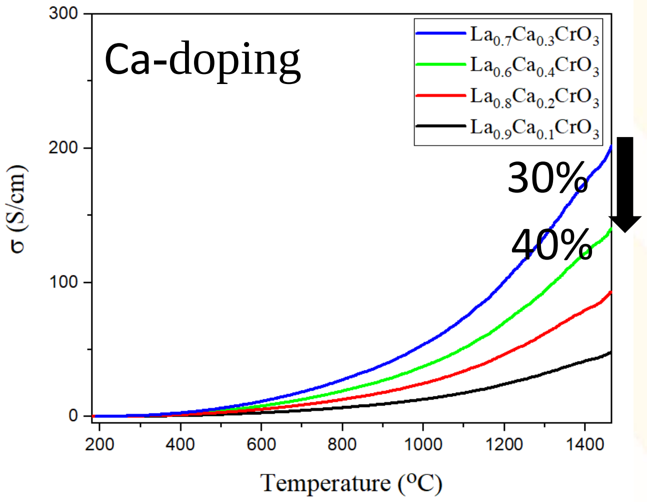

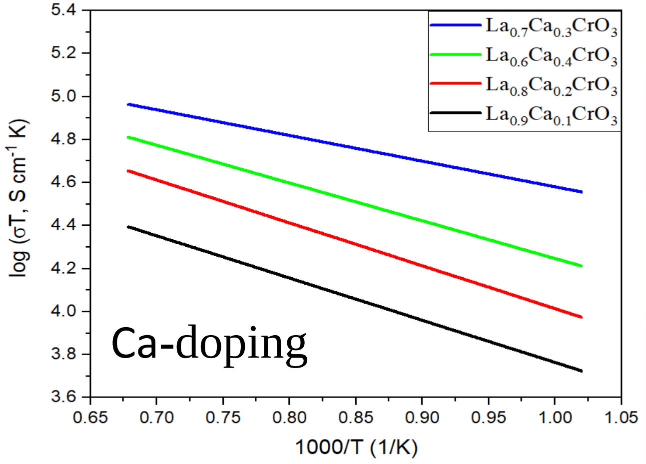

Electrical conductivity vs temperature and Arrhenius Plot $La_{1-x}Sr_xCrO_3$, $La_{1-x}Ca_xCrO_3$

- Conductivity typically exponentially increases with increase in carrier mobility, but 30 to 40% all drop in conductivity (believe slight second phase or higher lattice strain).
- Sr doped shows three regions, not seen in literature, since most tests <850°-1000°C. (believe V_o at high temperature)
- Arrhenius relationship fits for higher temperature regimes.
- Calcium doped compositions present higher conductivity due the lower distortion effects on lattice structure.

DC Electrical Conductivity (Reducing Atmosphere)

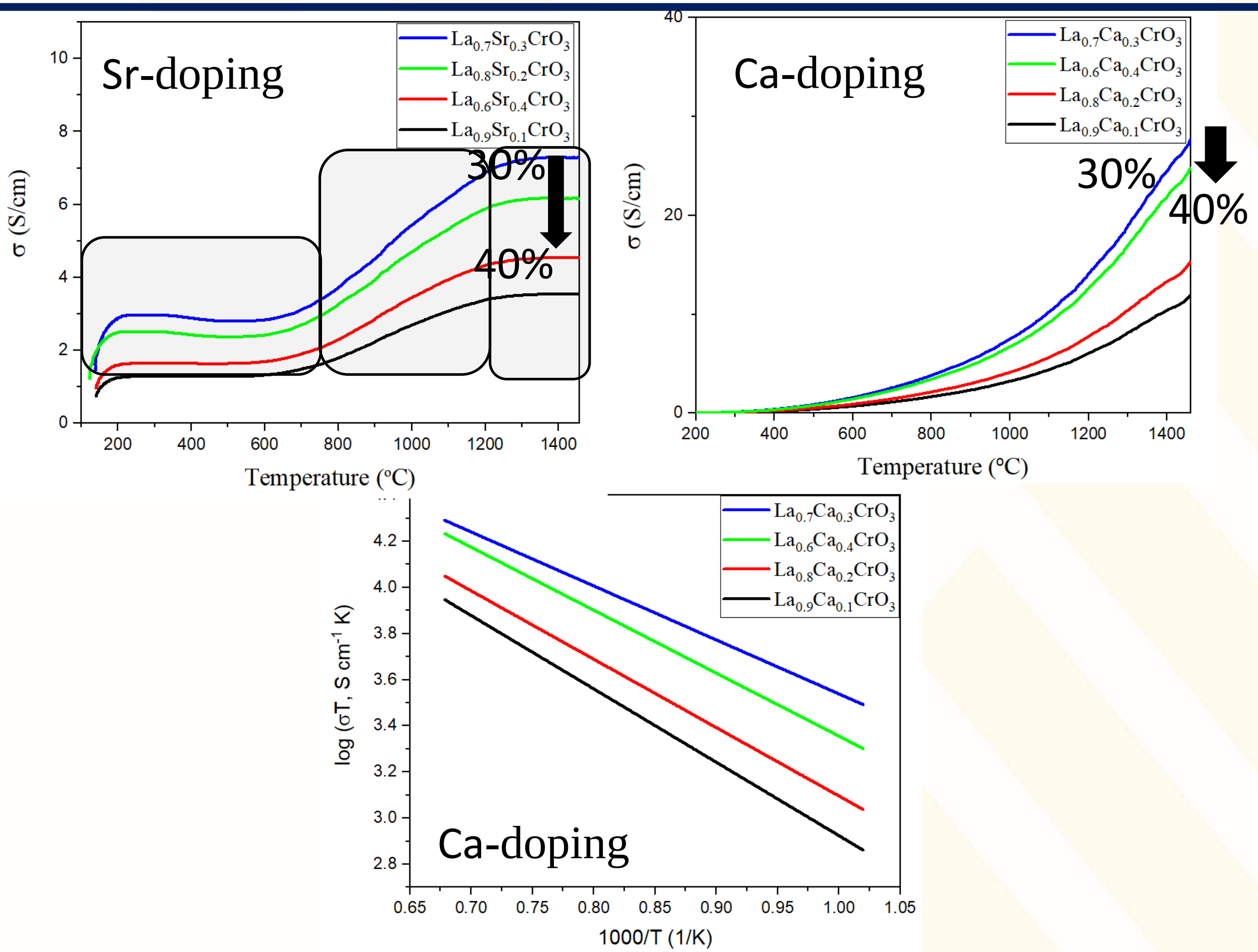

Electrical conductivity vs temperature and Arrhenius Plot for $La_{1-x}Sr_xCrO_3$, $La_{1-x}Ca_xCrO_3$

- Conductivity decrease for all temperature range under reducing atmosphere (H_2 5%/ N_2 95%).
- Under reducing conditions, oxygen vacancies form to keep neutrality (drop in hole carrier concentration).
- Sr conductivity still displays regions of altered mechanism.
- All compositions present lower conductivity as dopant increases (but still 40% lower than 30% in all cases).

Thick Film Sensors Fabrication

Thermoelectrical Characterization

West Virginia University

High Temperature Sensors Fabrication

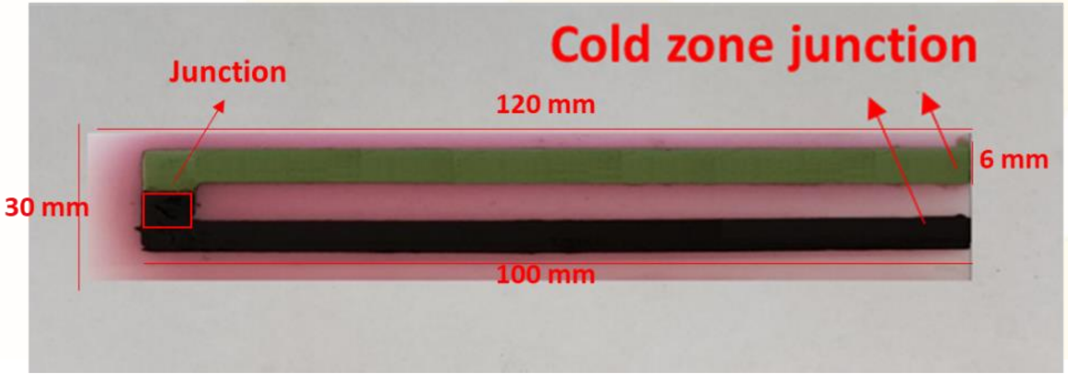

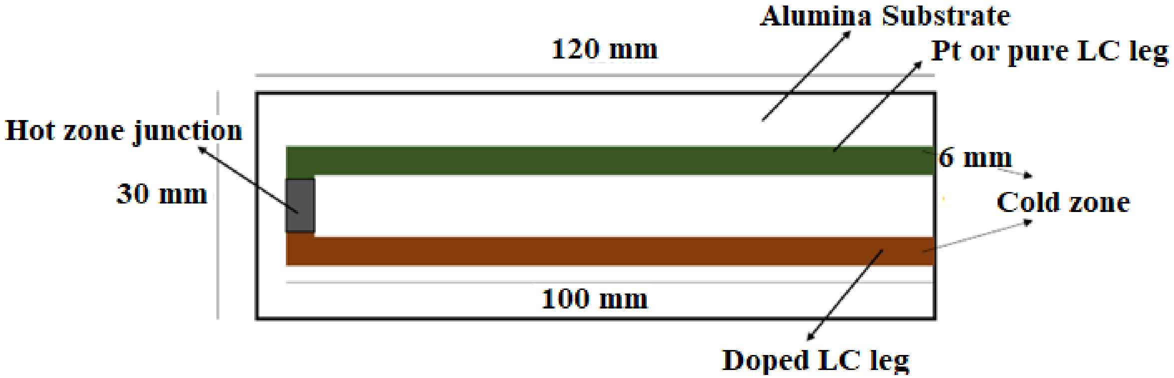

- Research team currently fabricating thermistors and thermocouples by 3D printing.
- High-temperature thermocouples that function >1200°C (in R-type range) new exciting development.

Leg 1 (Pt or pure-$LaCrO_3$)

Leg 2 (Doped $LaCrO_3$)

↓

Ball milling in isopropanol for 8 h and drying

↓

Ink preparation by mixing with an organic vehicle and ultrasonication

↓

3D printing on as-prepared alumina substrates (120 x 30 mm) and drying

↓

Sintering of the thermocouples (2°C/min, 1500°C, 1 h)

West Virginia University

Seebeck Coefficient Estimation (Using Pt Standard)

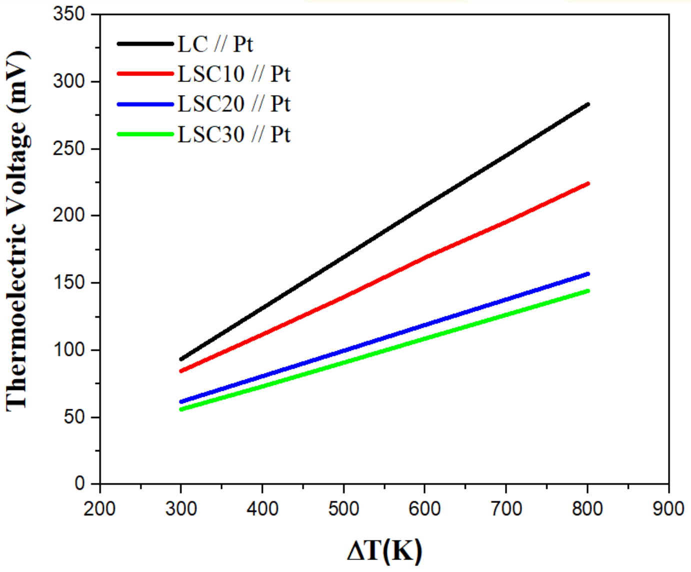

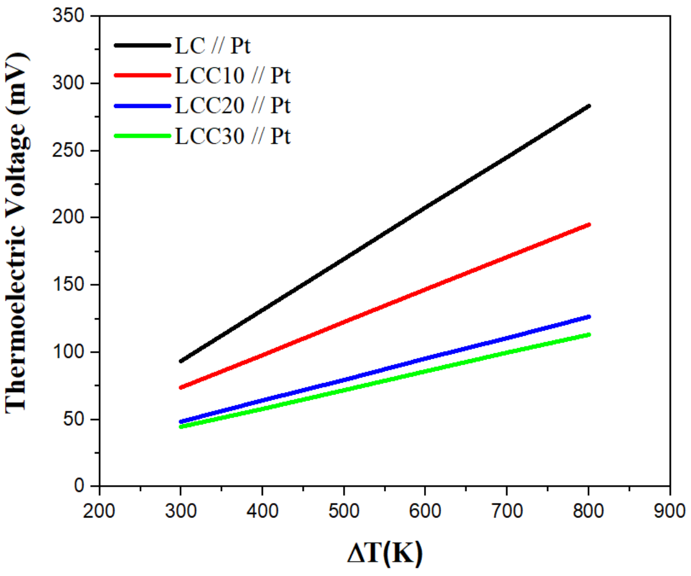

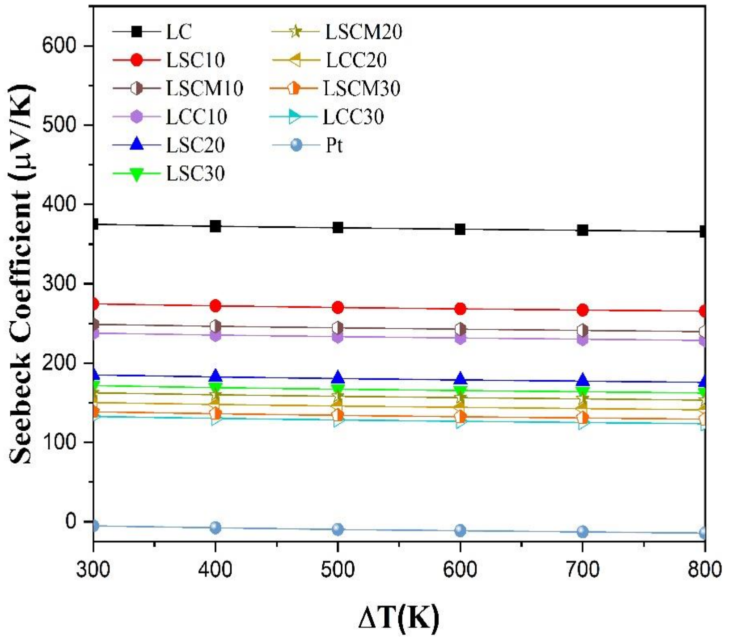

$$S(c) = (k_B/e)\ln[2(1-c)/c]$$

Heikes Equation

- Linear correlation between temperature difference and thermoelectric voltage was observed for all the compositions.
- Doped-$LaCrO_3$/Pt couples were fabricated to estimate absolute Seebeck coefficient (S_{Pt}~ -18 μV/K*) up to 1000°C.
- Ca doping shows lowest absolute Seebeck coefficient with increasing Ca content.

Thermoelectric Characterization of Thermocouples

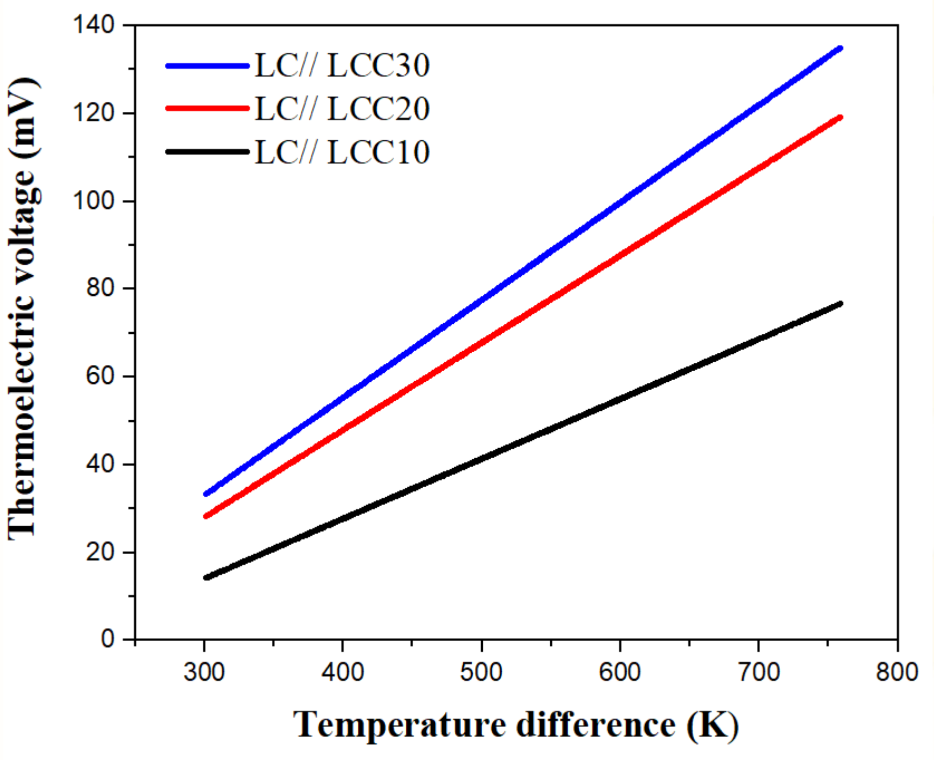

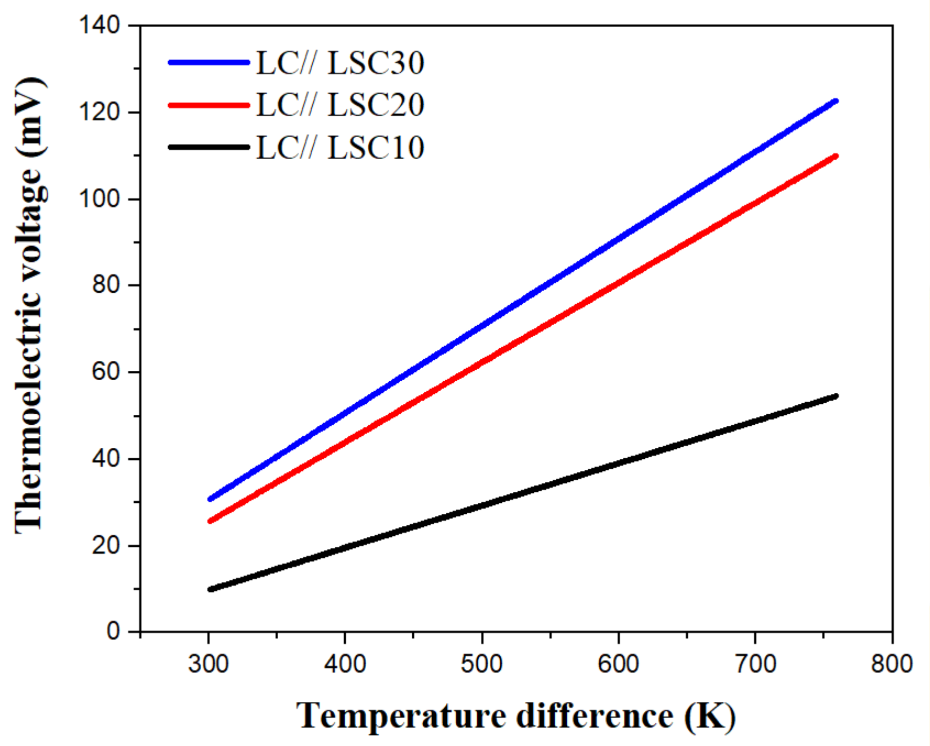

- Thermocouples were tested in a range between 30 to 850°C during 3 heating cycles, showing an excellent reproducibility.
- The LCC30/LC, LCC20/LC and LCC10/LC thermocouples showed a maximum higher voltage by **two orders of magnitude in comparison with Pt/Pt-Rh**, with values of 138.61 mV, 119.50 mV and 79.10 mV respectively (at ΔT~750°C).

Sensors Embedded into Refractory

West Virginia University

Embedded Sensors Fabrication

General Smart Refractory Processing Method

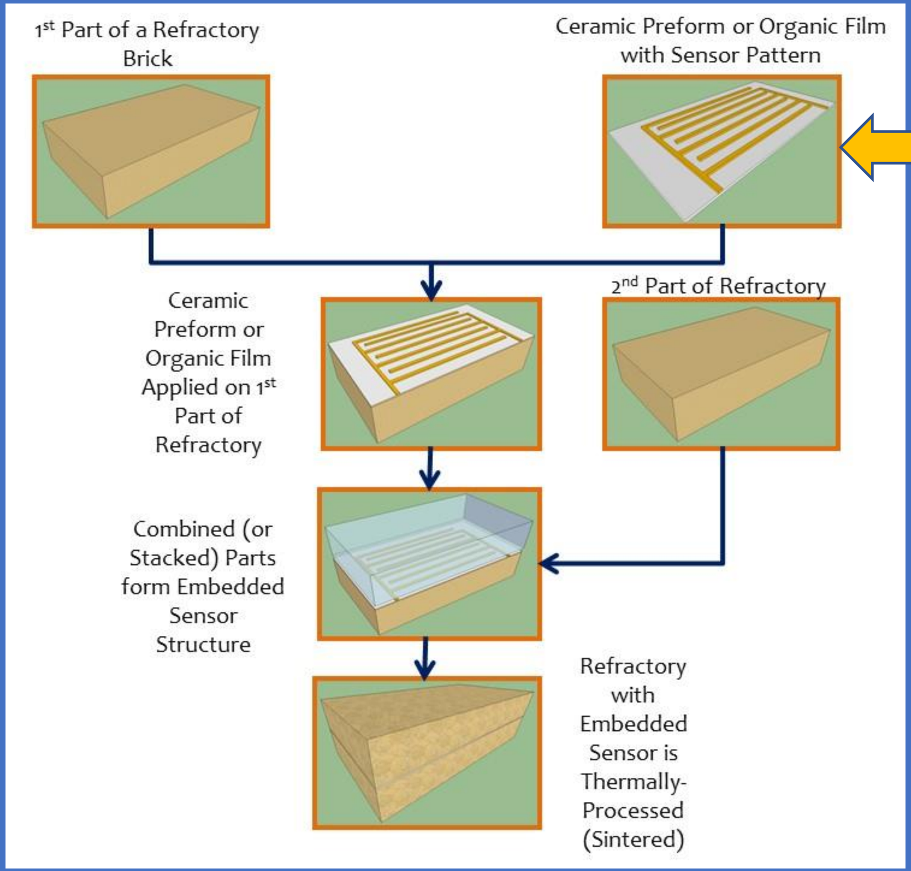

Examples of Sensor Preforms

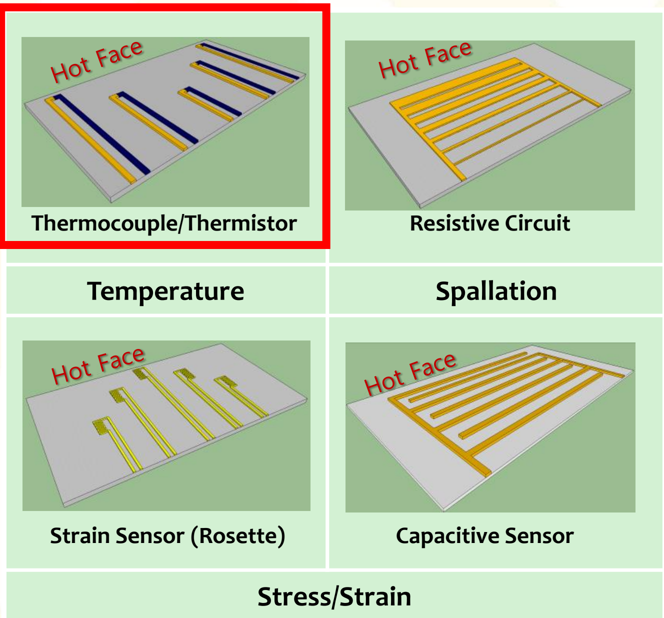

Embedded Thermocouples Characterization

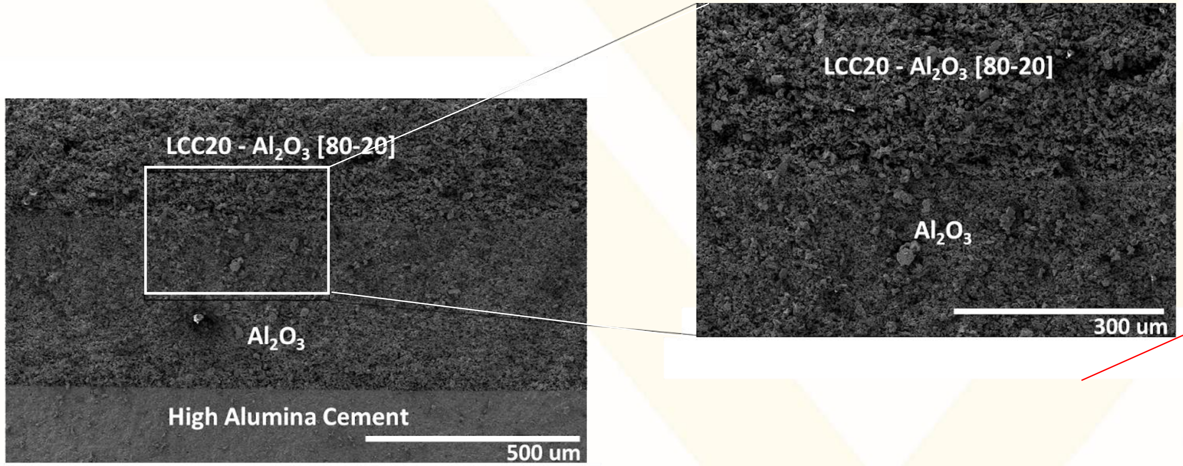

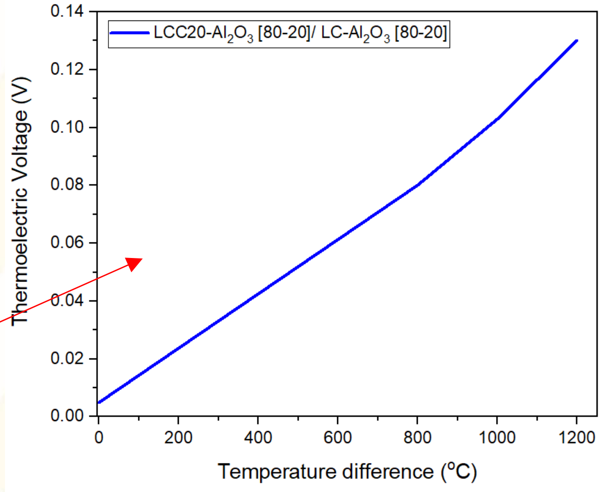

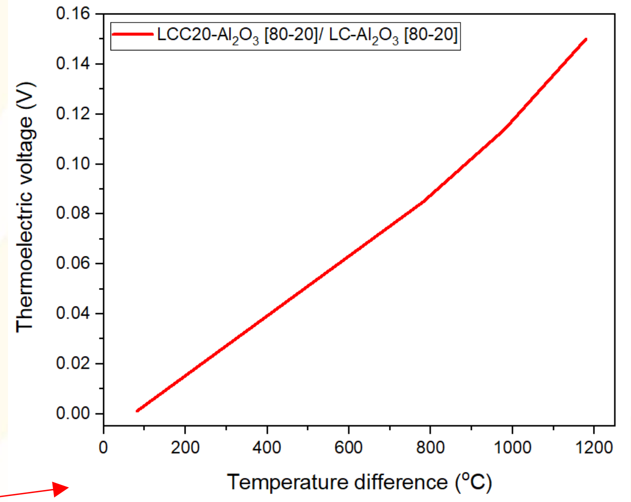

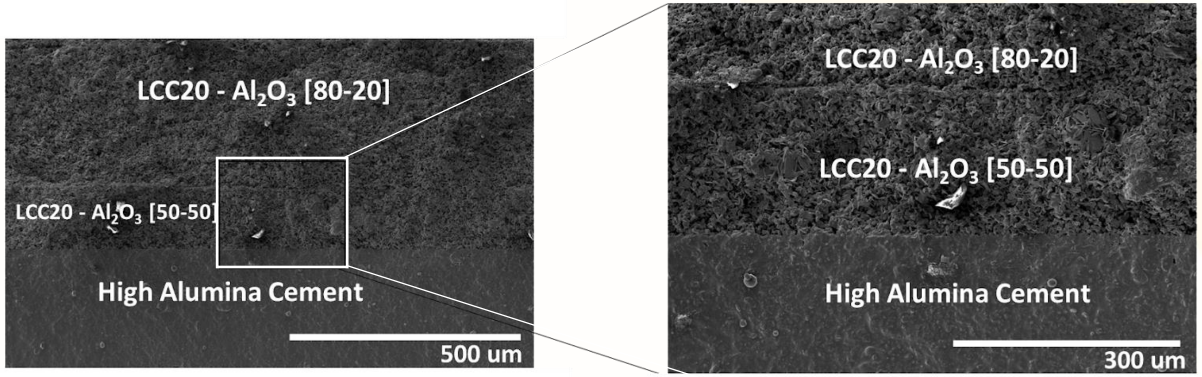

- Different 3D printing gradients were printed and embedded into high alumina refractory cement.
- Embedded thermocouples showed thermoelectric voltage responses ~ 0.15 V in at ΔT~1200°C

WestVirginiaUniversity

Embedded Sensors
Initial Corrosion Testing

Corrosion Testing of Embedded Sensors

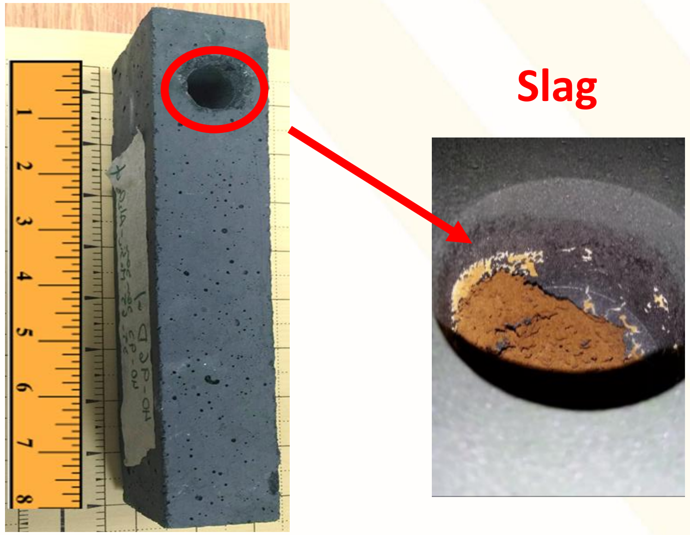

Slag

Chromia refractory bricks

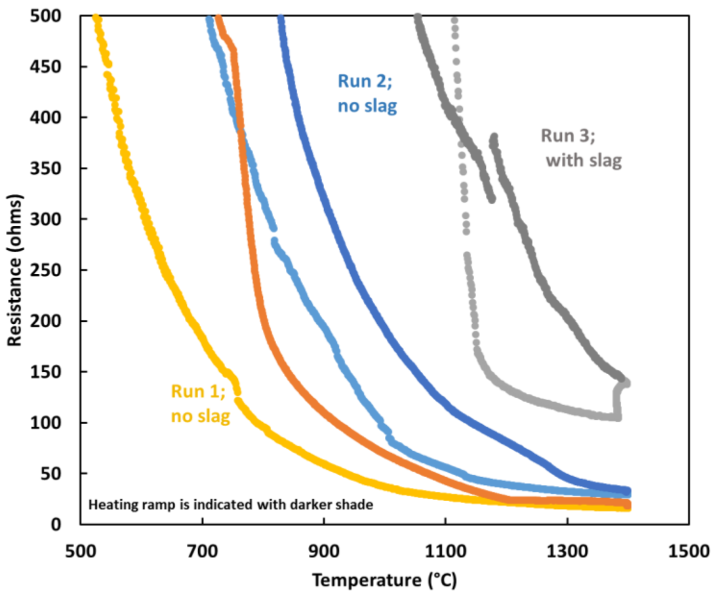

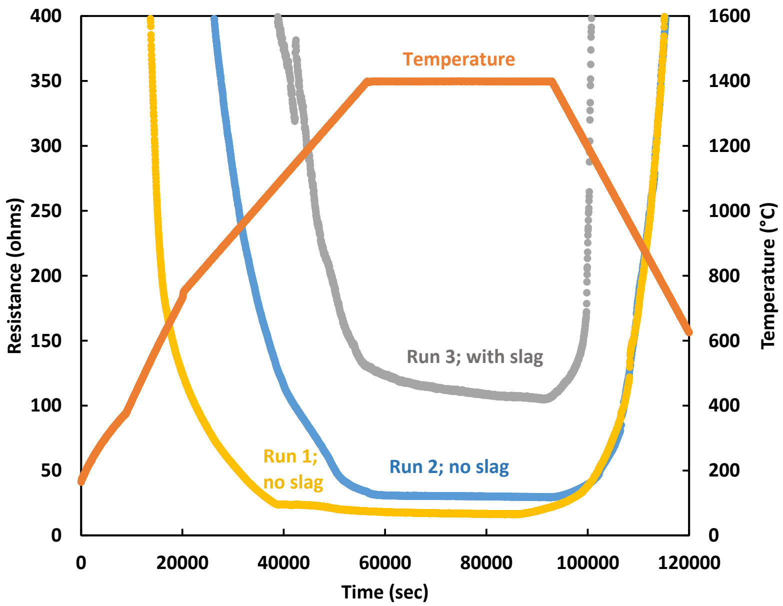

- Resistance and temperature profile and resistance versus time, respectively, for brick containing LNO (coarse) thermistor tested to 1400°C for 10 hrs.
- The brick was cycled between room temperature and 1400°C two times without slag. Before third run, 32 grams of slag pellets were added.
- With each thermal cycle, the resistance at each hold appears to increase, while it still shows slight decrease during the hold as shown with data collected with preforms.

Conclusions

Conclusions

- Electrical conductivity shows correlated dependence with high temperature (up to 1500ºC) for all compositions. The exponential Arrhenius trend is evidence for the polaron hopping electrical conduction mechanism.

- All the Seebeck coefficients were determined as the slope of the obtained plots, observing constant behavior as expected for polaron hopping active semiconductors such as doped $LaCrO_3$.

- It was observed that Seebeck coefficient reduces with the increase in dopant substituents as expected by Heikes model.

- Chromium diffusion was observed, there is a necessity for protect conductive layers and reduce chromium lost.

Conclusions

- Embedded thermocouples into oxide refractories were fabricated using an easy approach.

- The embedded thermocouples showed a correlated increase in thermoelectric voltage (as expected) in function of temperature difference increment.

- The change in resistance of the embedded thermocouples in time can be related to platinum connections at high temperatures and multiple testing.

Acknowledgment

- We would like to thank U.S. Department of Energy (DOE) and Maria Reidpath (project manager) for sanctioning this project DE-FE0031825.

- We also would like to acknowledge Mr. Harley Hart, Dr. Qiang Wang, and Dr. Marcela Redigolo for their cooperation and valuable assistance in the WVU Shared Research Facilities (SRF).

- We also would like to thank HWI, for support us in developing real-life applications sensing systems/devices.

- Kindly acknowledge faculty and staff of West Virginia University for their support.

Thank you for the attention.

Email: jam00009@mix.wvu.edu
Email: Ed.Sabolsky@mail.wvu.edu

West Virginia University

Electrical Conductivity (Oxygen partial pressure)

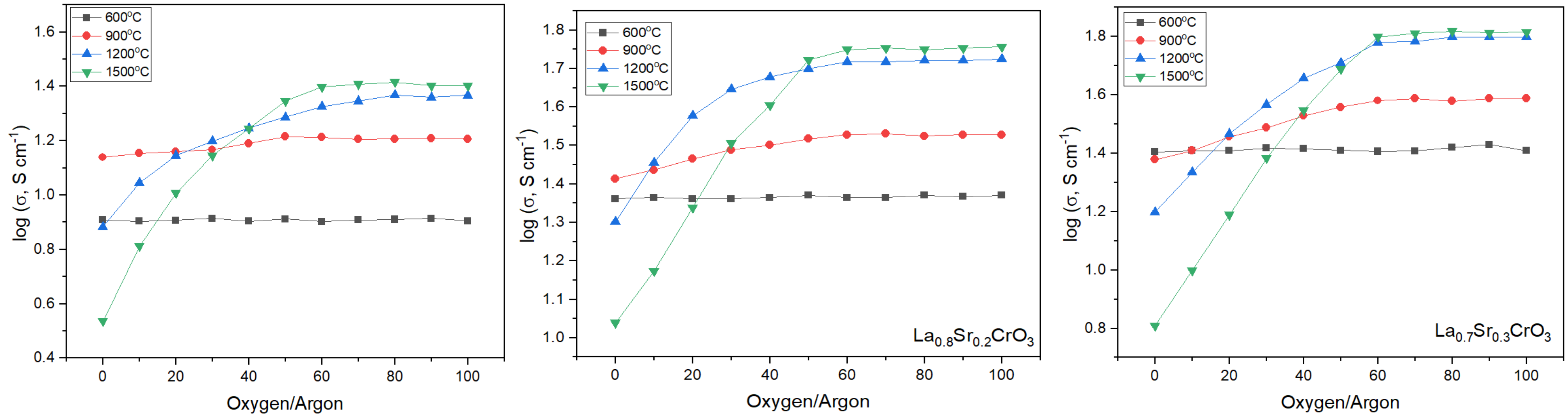

Electrical conductivity dependence of oxygen partial pressures at different temperatures for $La_{1-x}Sr_xCrO_3$

- ❖ At lower temperatures (600ºC - 900ºC) not significant changes in conductivity occurs for lanthanum doped compositions during the equilibrium time used (90 minutes).
- ❖ At higher temperatures (1200ºC and 1500ºC) the conductivity drops exponentially at lower oxygen partial pressures. Increasing the strontium concentration, the conductivity drop significantly.

Electrical Conductivity (Oxygen partial pressure)

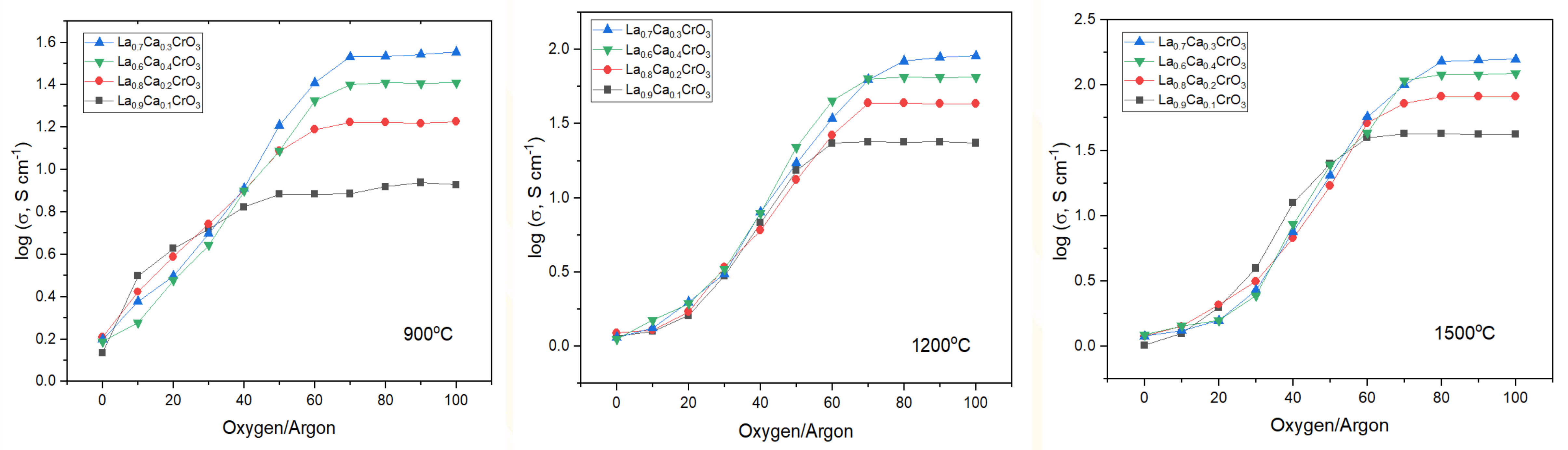

Electrical conductivity dependence of oxygen partial pressures at different temperatures for $La_{1-x}Ca_xCrO_3$

- ❖ When the oxygen partial pressure goes below a critical value, the oxygen vacancies are generated at expense of electron holes and conductivity decrease for all compositions.
- ❖ The charge imbalance caused by the introduction of Calcium starts to be compensated by the formation of oxygen vacancies.

Sr doped lanthanum chromite stability experiments

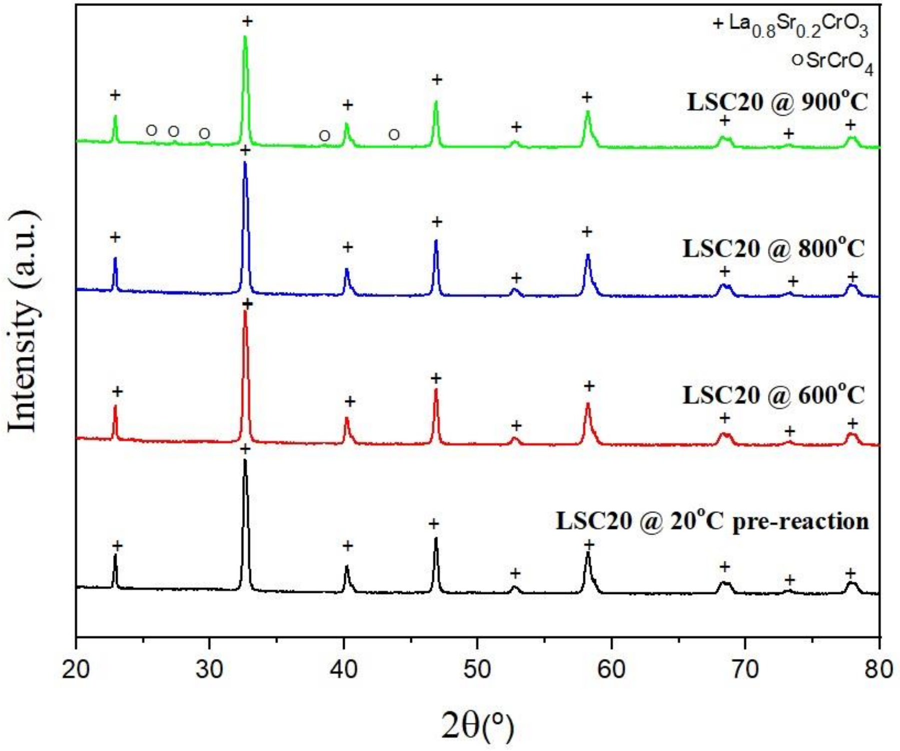

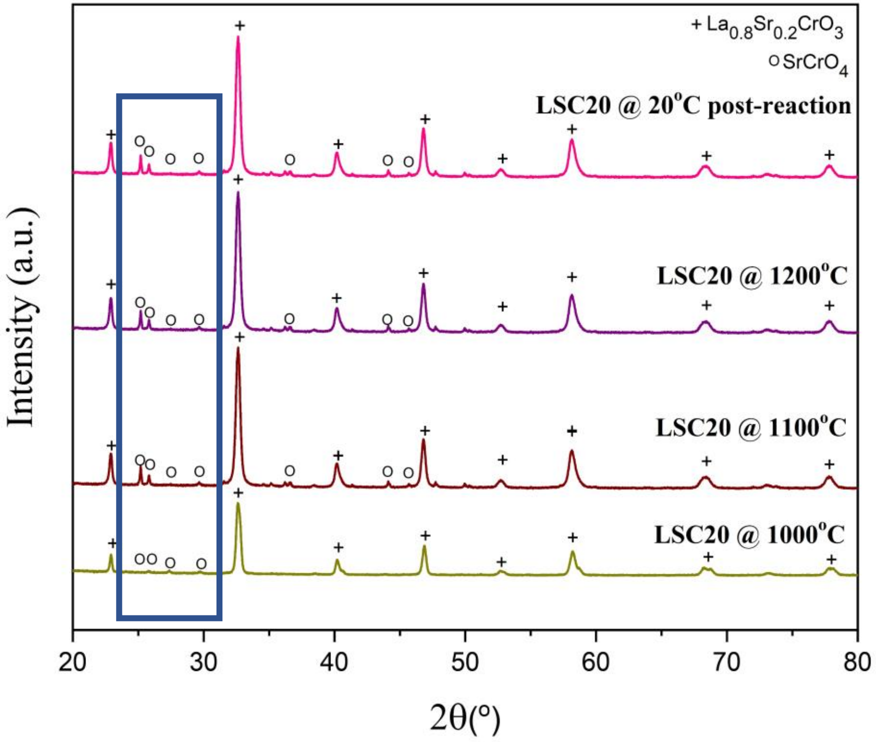

X-ray diffractograms of 20% strontium doped lanthanum chromite annealed at different temperatures.

Crystalline Structure/Phase Analysis

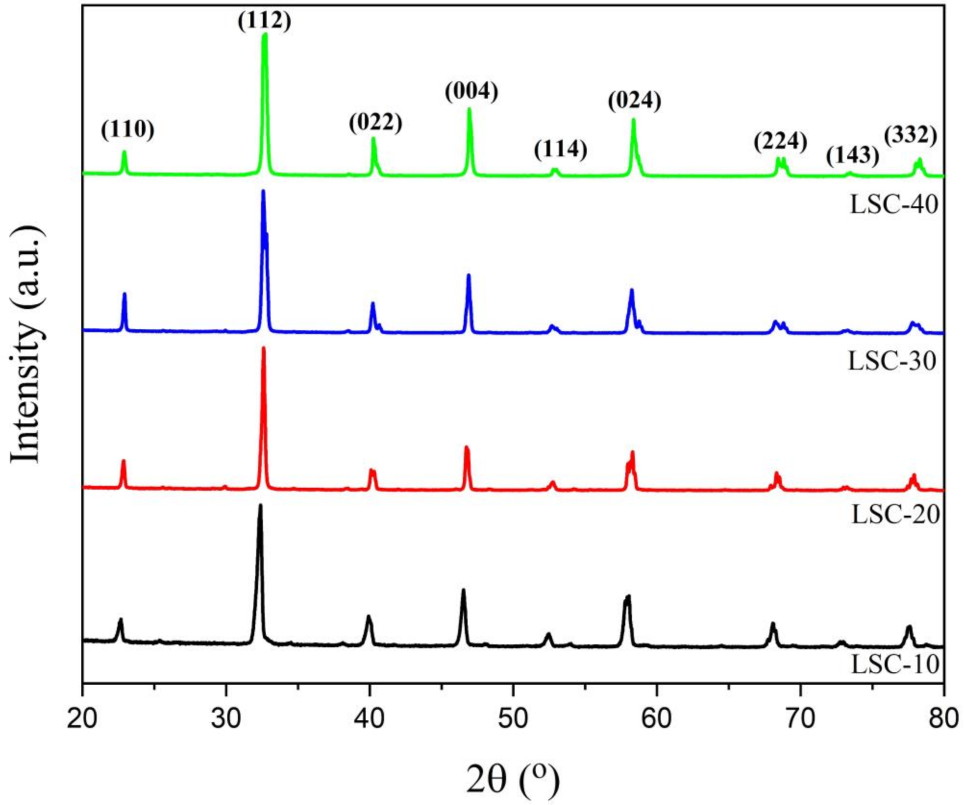

X-ray diffractograms for the samples of the $La_{1-x}Sr_xCrO_3$ series

- Single phase doped lanthanum chromites materials were obtained successful (no residual oxide or pyrochlore peaks).
- Using Pechini Sol-Gel method permitted doped lanthanum chromites at high solubility levels (40%).
- Solubility limits >40% substitution level (Sujatha *et al.* 1992).
- No impurities extra peaks were present in the final prepared powders and ceramic pellets.

Lattice Parameters, Unit Cell Volume and Density

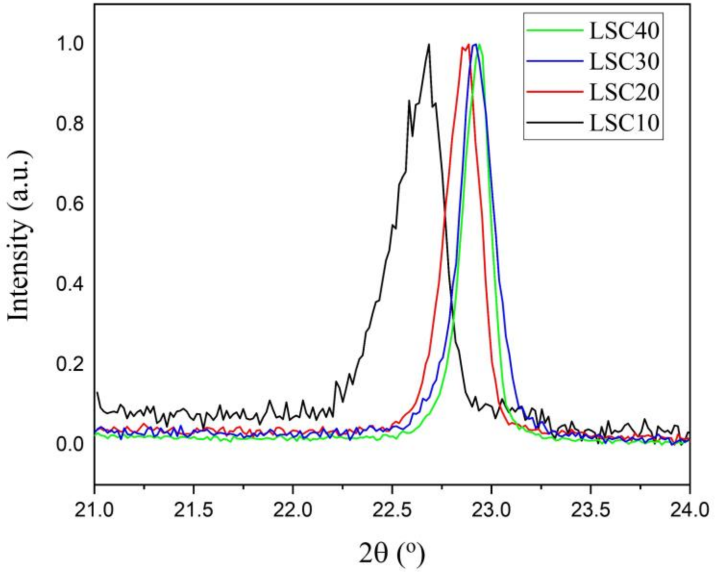

X-ray diffractograms showing shifting of (110) peak for the $La_{1-x}Sr_xCrO_3$ series

Lattice parameters, unit cell volume and XRD theoretical density for doped lanthanum chromites perovskites

Composition	Lattice parameters (Å) a	b	c	Volume ($Å^3$)	$\rho XRD_{Theoretical}$ (g/cm^3)
$La_{0.9}Sr_{0.1}CrO_3$	5.5124	5.5668	7.7926	239.1299	6.4932
$La_{0.8}Sr_{0.2}CrO_3$	5.4988	5.5425	7.7853	237.2747	6.4004
$La_{0.7}Sr_{0.3}CrO_3$	5.4769	5.5233	7.7580	234.6839	6.3259
$La_{0.6}Sr_{0.4}CrO_3$	5.4524	5.5122	7.7407	232.6441	6.2350
$La_{0.9}Ca_{0.1}CrO_3$	5.4180	5.5039	7.7332	230.6050	6.5963
$La_{0.8}Ca_{0.2}CrO_3$	5.4092	5.4982	7.7264	229.7898	6.3341
$La_{0.7}Ca_{0.3}CrO_3$	5.3994	5.4877	7.7058	228.3264	6.0872
$La_{0.6}Ca_{0.4}CrO_3$	5.3897	5.4622	7.6853	226.2520	5.8528
$La_{0.8}Sr_{0.20}Cr_{0.90}Mn_{0.10}O_3$	5.4734	5.5648	7.7765	236.8595	6.1533
$La_{0.8}Sr_{0.20}Cr_{0.80}Mn_{0.20}O_3$	5.4705	5.5587	7.7702	236.2829	6.1766
$La_{0.8}Sr_{0.20}Cr_{0.70}Mn_{0.30}O_3$	5.4598	5.5398	7.7498	234.4020	6.2344
$La_{0.8}Sr_{0.20}Cr_{0.60}Mn_{0.40}O_3$	5.4146	5.4981	7.7065	229.4225	6.3783

%Sr↑

%Ca↑

%Mn↑

- Decrease in lattice parameters (and volume) were observed when dopant cations is introduced in the lattice.
- To achieve neutrality chromium change from Cr^{+3} to Cr^{+4}, reduction in the chromium size occurs (Hyun Choi *et al.* 2013) .

Microstructure/Grain Size Distribution

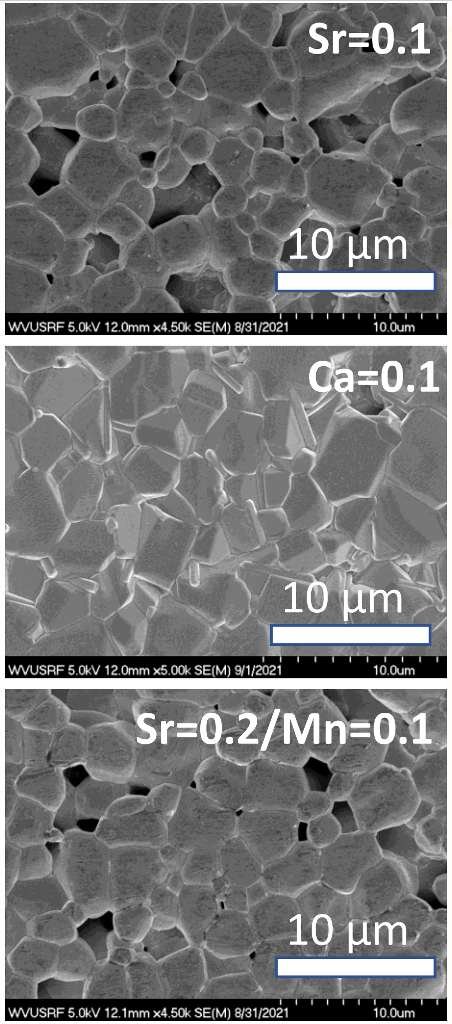

Average grain size and bulk density distribution for $La_{1-x}Sr_xCrO_3$, $La_{1-x}Ca_xCrO_3$ series

Composition	Average Grain Size (µm)	Relative Percentage Bulk Density (%)	
$La_{0.9}Sr_{0.1}CrO_3$	3.6	94	%Sr↑
$La_{0.8}Sr_{0.2}CrO_3$	3.5	95	
$La_{0.7}Sr_{0.3}CrO_3$	3.6	95	
$La_{0.6}Sr_{0.4}CrO_3$	3.2	94	
$La_{0.9}Ca_{0.1}CrO_3$	4.1	96	%Ca↑
$La_{0.8}Ca_{0.2}CrO_3$	3.7	97	
$La_{0.7}Ca_{0.3}CrO_3$	3.7	97	
$La_{0.6}Ca_{0.4}CrO_3$	3.6	98	

- Pechini Sol Gel prepared calcium, strontium, manganese doped lanthanum chromite powders exhibit better sinterability and densification under oxidizing conditions (undoped ↓90%).
- The samples of Ca doped lanthanum chromite powder have more dense microstructures. Furthermore, it was found that the incorporation of Ca, Sr in the A site of the lanthanum chromite increases grain growth (undoped <3 µm).

DC Electrical Conductivities/Activation Energies

Composition	Air Atmosphere		Reducing Atmosphere	
	Conductivity @ 1000°C (S/cm)	Activation energy (eV)	Conductivity @ 1000°C (S/cm)	Activation energy (eV)
$La_{0.9}Sr_{0.1}CrO_3$	16.672	0.1552	2.691	0.3238
$La_{0.8}Sr_{0.2}CrO_3$	42.882	0.1427	4.572	0.2597
$La_{0.7}Sr_{0.3}CrO_3$	49.032	0.1055	5.534	0.1719
$La_{0.6}Sr_{0.4}CrO_3$	23.599	0.1498	3.462	0.3102
$La_{0.9}Ca_{0.1}CrO_3$	13.211	0.1417	3.152	0.3240
$La_{0.8}Ca_{0.2}CrO_3$	24.170	0.1298	4.118	0.2103
$La_{0.7}Ca_{0.3}CrO_3$	52.823	0.1028	7.602	0.1367
$La_{0.6}Ca_{0.4}CrO_3$	38.152	0.1175	6.626	0.1747

$$\sigma = \frac{\sigma_0}{T} \exp\left(\frac{-\Delta E_a}{kT}\right)$$

Slope $\propto E_a$

- ❖ Conductivity increase as function of doping level up to 30% for all dopants (strontium, calcium and manganese).
- ❖ At 40% doping levels conductivity decrease due to higher lattice distortion in all systems (solubility limit).
- ❖ Lower conductivity values under reducing atmospheres are explained by oxygen vacancies formation (near >1.5× in activation energy).

West Virginia University

Ca doped lanthanum chromite stability experiments

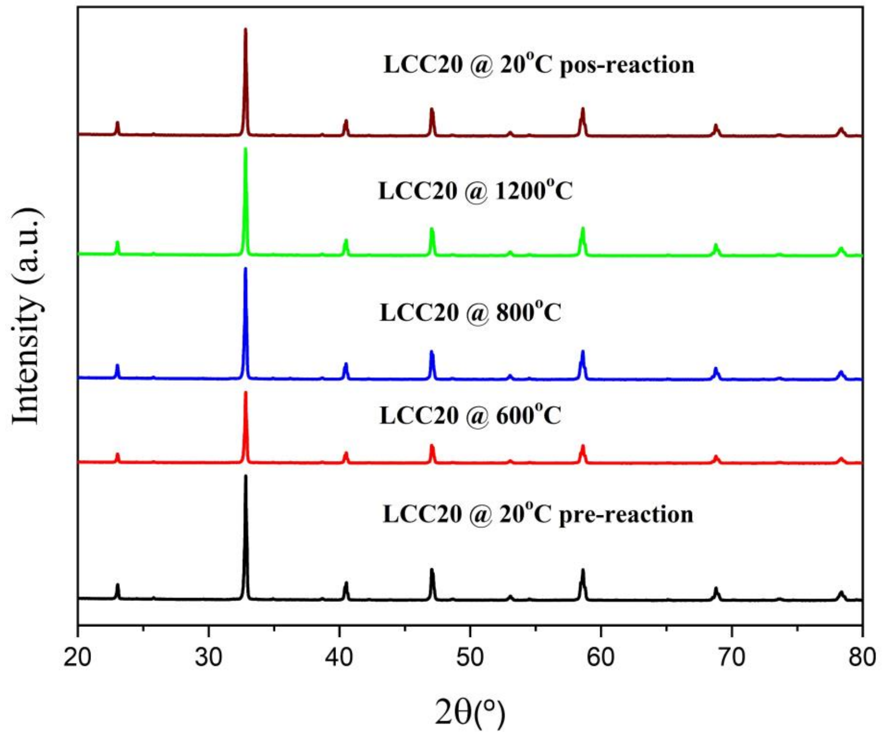

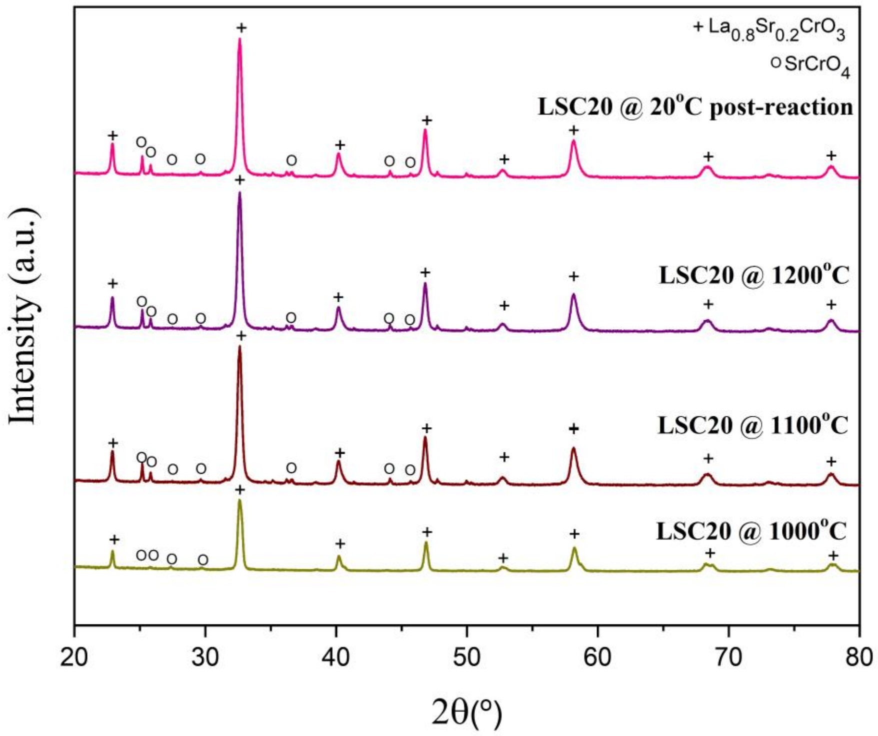

X-ray diffractograms of 20% strontium and calcium doped lanthanum chromite annealed at different temperatures.

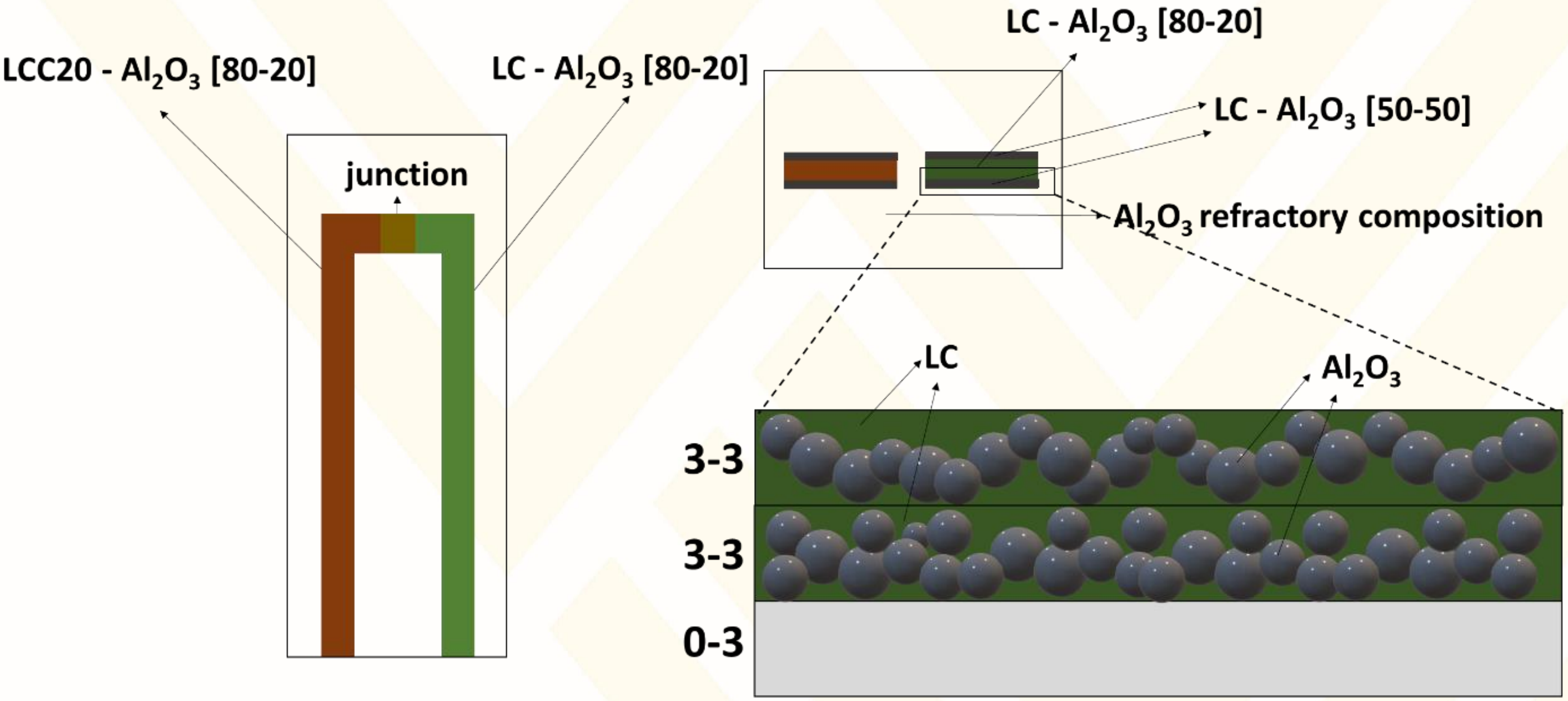

West Virginia University

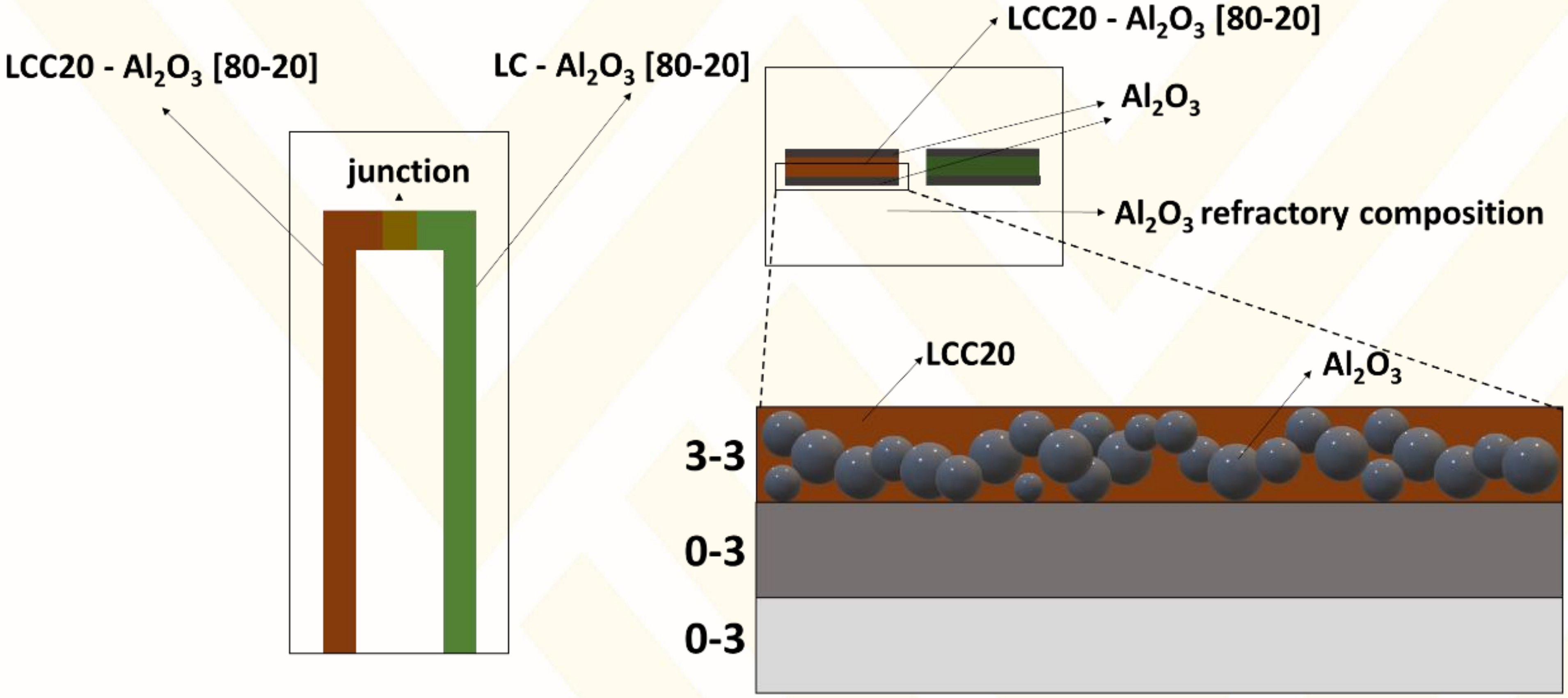
LCC20 - Al_2O_3 [80-20]
LC - Al_2O_3 [80-20]
junction
LCC20 - Al_2O_3 [80-20]
Al_2O_3
Al_2O_3 refractory composition
LCC20
Al_2O_3
3-3
0-3
0-3

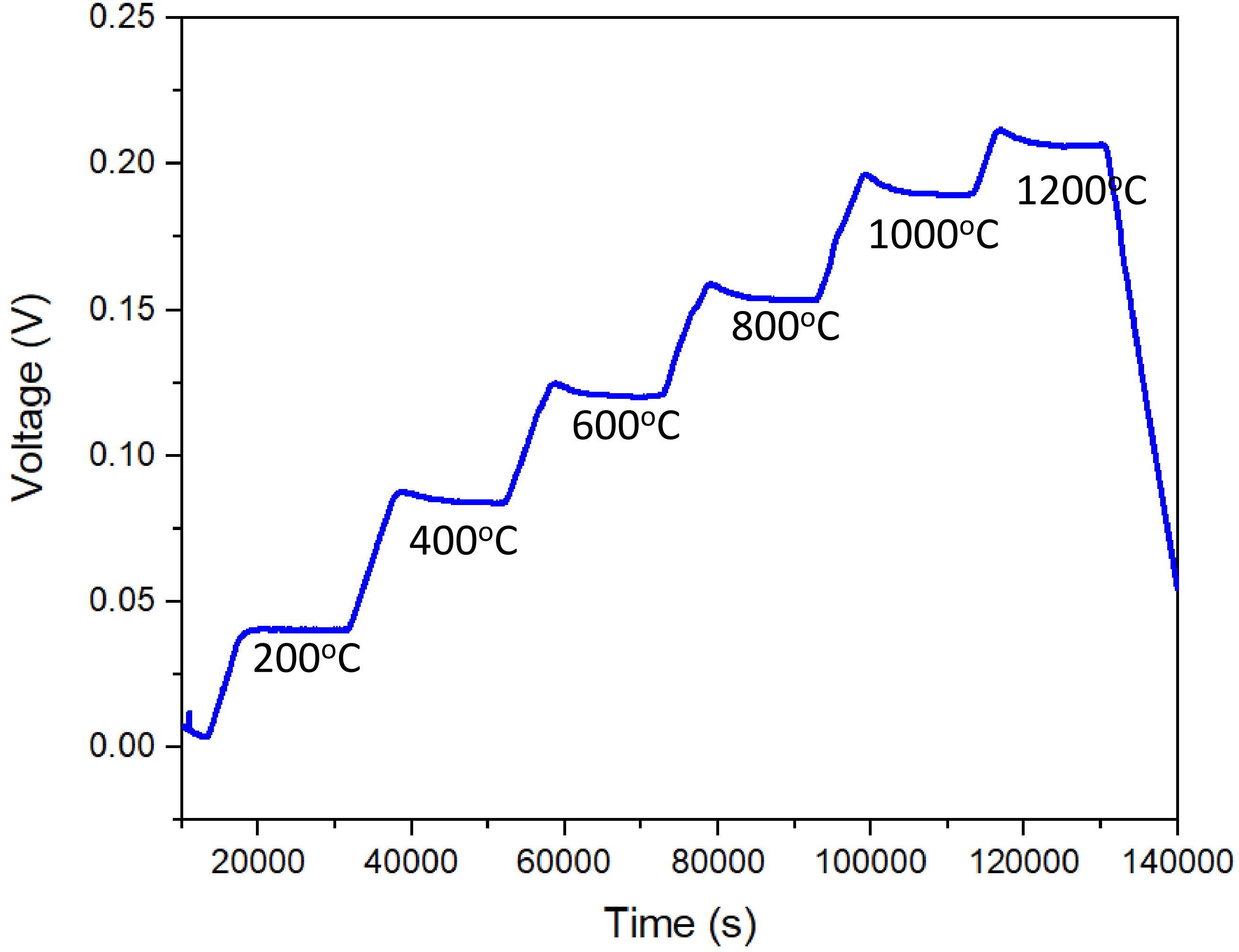

1 Alumina layer
1 LCC/ Alumina 95/5 layer
1 Alumina layer

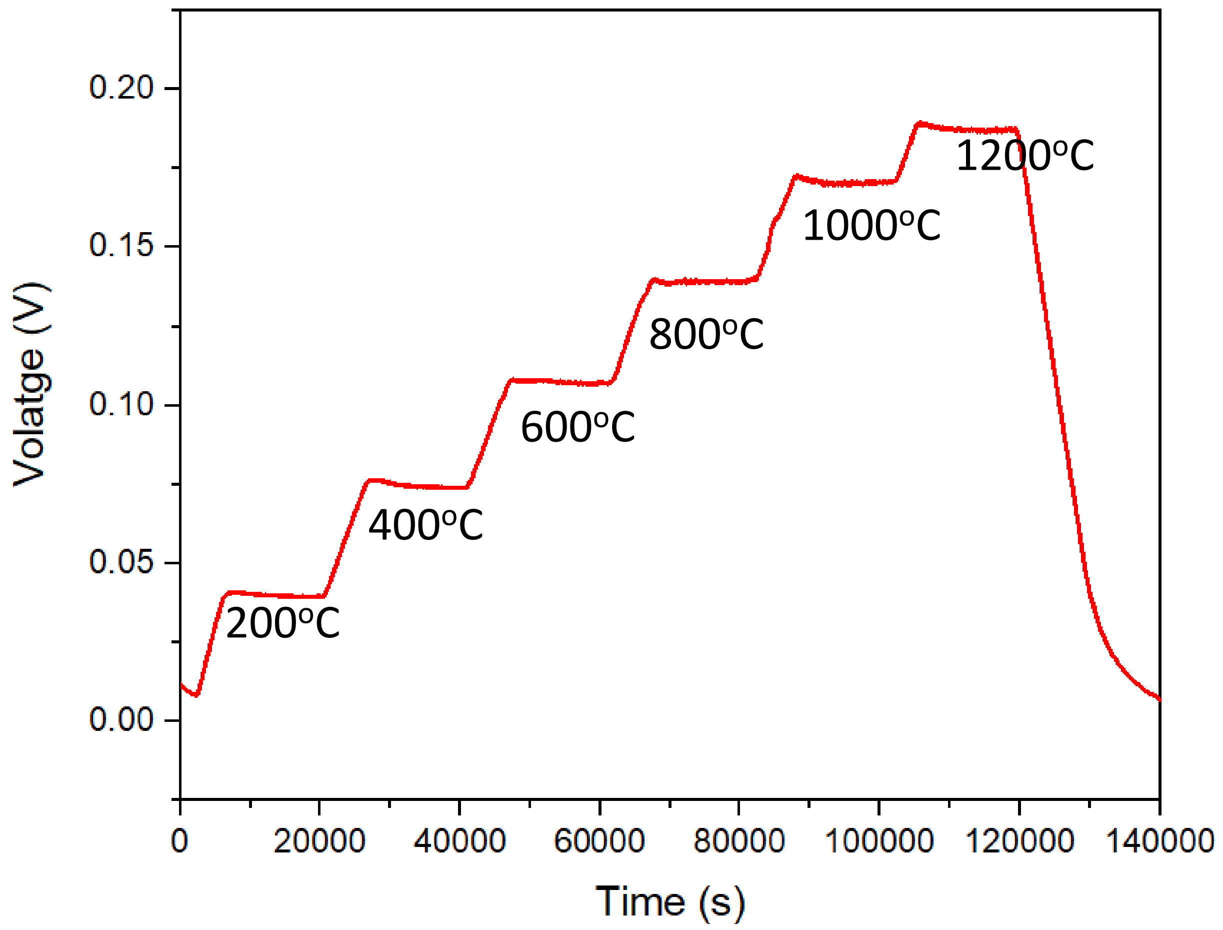

2 layers LCC20
2 Layers LC

XRD - Composites characterization

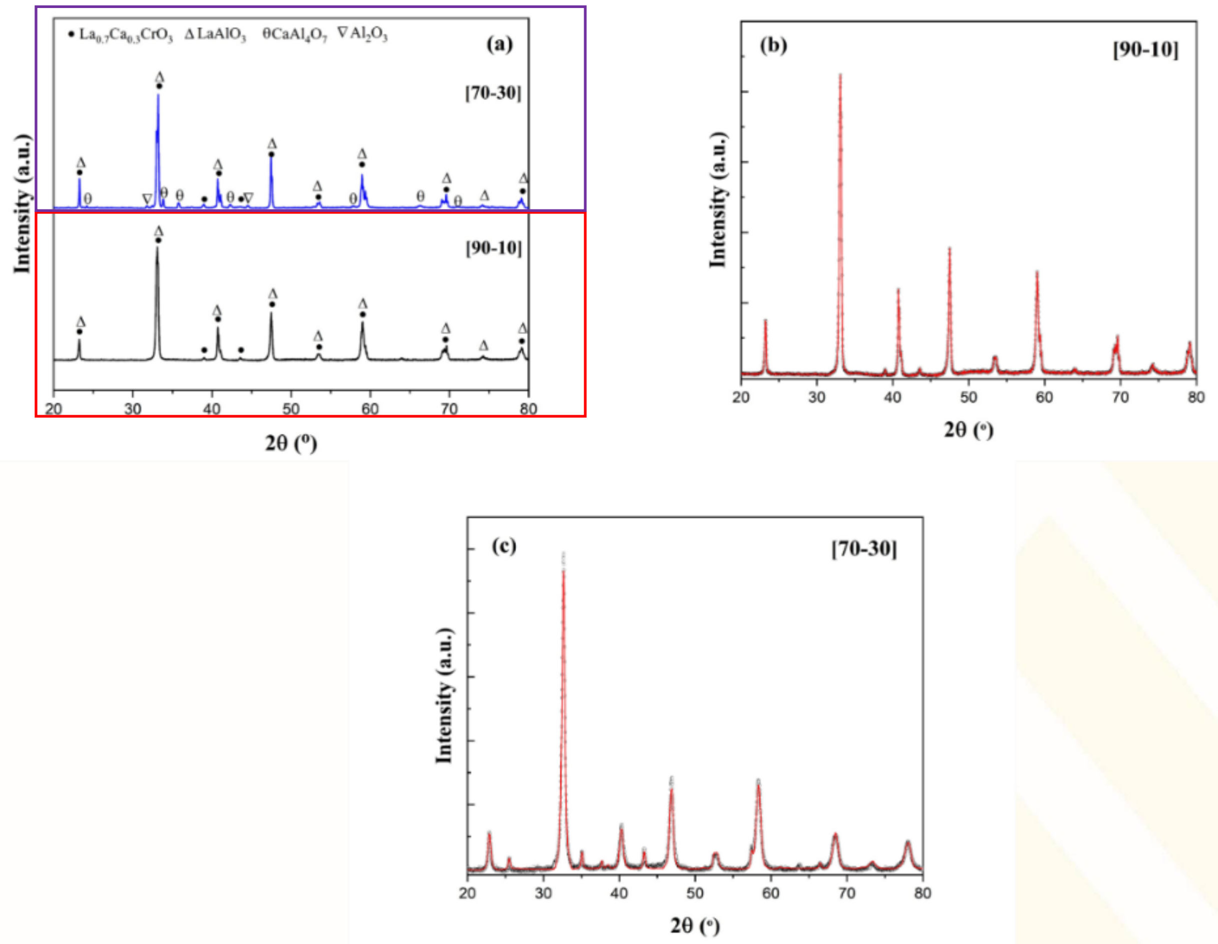

- LCC30-Al_2O_3 [90-10] indicates that LCC30 phase was present, and a secondary lanthanum aluminate was formed during the sintering process.
- LCC30-Al_2O_3 [70-30] diffractogram shows LCC30 and lanthanum aluminate ($LaAlO_3$), calcium aluminate ($Ca_2Al_2O_5$) and pure Al_2O_3.
- Increasing the Al_2O_3 volume content in the composite, increase the chemical reactivity at 1500^{o}C.

SEM - Composites characterization

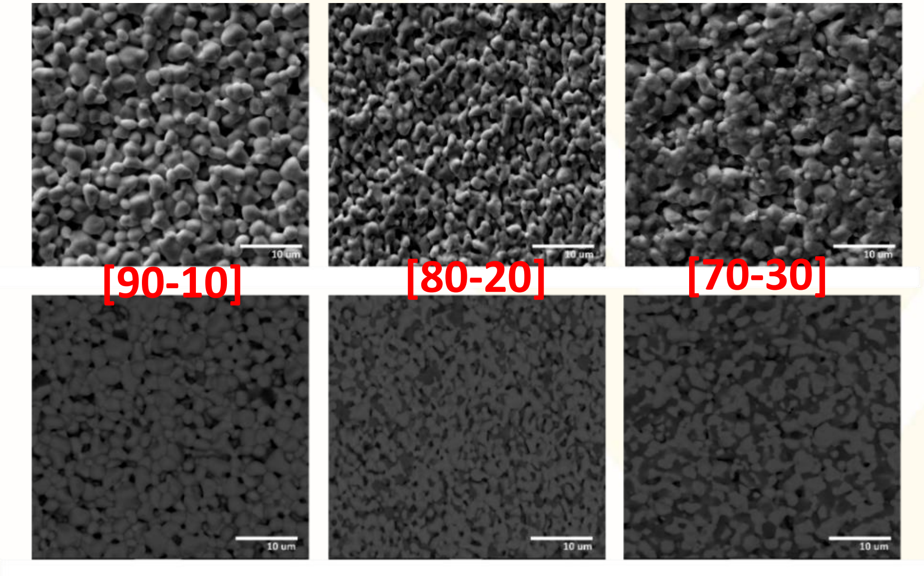

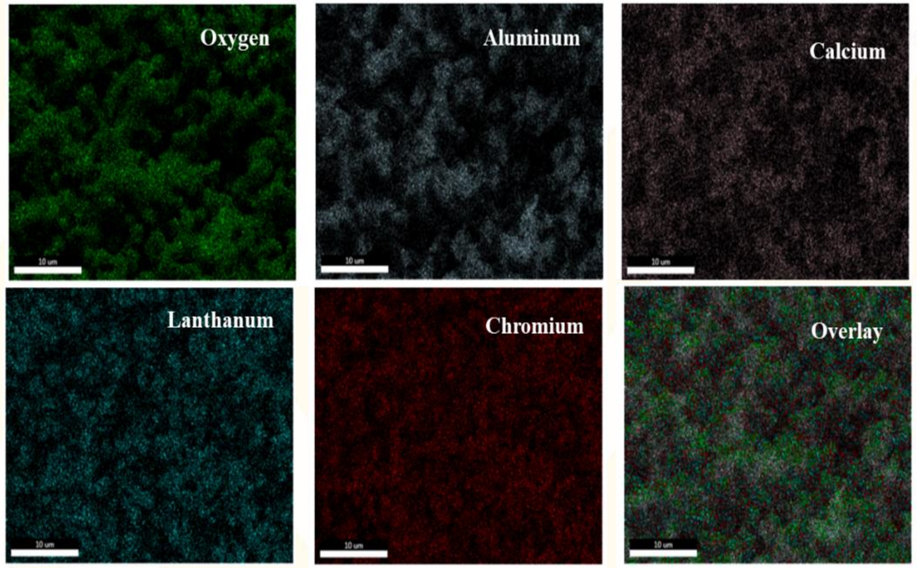

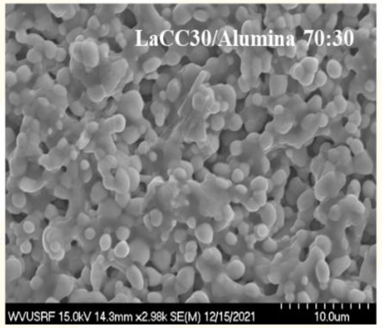

- At 10 vol% of Al_2O_3 there is not connectivity between grains indicating the formation of a (3-0) composite.
- At 20 vol% and 30 vol% the connectivity of the grains is more notable, indicating the formation of (3-3) composites.
- These results demonstrated that the degree of percolation of Al_2O_3, $LaAlO_3$ and $Ca_2Al_2O_5$ grain size increased by increasing Al_2O_3 content from 10 to 30 vol%.

West Virginia University